

Landform degradation and slope processes on Io: The Galileo view

Jeffrey M. Moore,¹ Robert J. Sullivan,² Frank C. Chuang,³ James W. Head III,⁴
Alfred S. McEwen,⁵ Moses P. Milazzo,⁵ Brian E. Nixon,⁴ Robert T. Pappalardo,^{4,6}
Paul M. Schenk,⁷ and Elizabeth P. Turtle⁵

Abstract. The Galileo mission has revealed remarkable evidence of mass movement and landform degradation on Io. We recognize four major slope types observed on a number of intermediate resolution (~ 250 m pixel⁻¹) images and several additional textures on very high resolution (~ 10 m pixel⁻¹) images. Slopes and scarps on Io often show evidence of erosion, seen in the simplest form as alcove-carving slumps and slides at all scales. Many of the mass movement deposits on Io are probably mostly the consequence of block release and brittle slope failure. Sputtering plays no significant role. Sapping as envisioned by *McCauley et al.* [1979] remains viable. We speculate that alcove-lined canyons seen in one observation and lobed deposits seen along the bases of scarps in several locations may reflect the plastic deformation and “glacial” flow of interstitial volatiles (e.g., SO₂) heated by locally high geothermal energy to mobilize the volatile. The appearance of some slopes and near-slope surface textures seen in very high resolution images is consistent with erosion from sublimation-degradation. However, a suitable volatile (e.g., H₂S) that can sublime fast enough to alter Io’s youthful surface has not been identified. Disaggregation from chemical decomposition of solid S₂O and other polysulfur oxides may conceivably operate on Io. This mechanism could degrade landforms in a manner that resembles degradation from sublimation, and at a rate that can compete with resurfacing.

1. Introduction

Mass movement and landform degradation reduces topographic relief by moving surface materials to a lower gravitational potential. Landform degradation commonly involves a reduction in material strength (e.g., loss or weakening of an interparticle binding agent or decrease in mechanical strength allowing disintegration or plastic deformation) and transport of this material under the influence of gravity. The identification of specific landform types associated with mass movement and landform degradation permits inferences about local sediment particle size and abundance, the nature of the binding cement, and transportation processes. Generally, mass movements on Earth can be classified in terms of the particle sizes and the speed of the material moved during transport [*Sharpe*, 1939; *Varnes*, 1958, 1978; *Coates*, 1977].

Such classification schemes have been used to characterize mass movements on Mercury, Venus, the Moon, Mars, and the Galilean satellites [e.g., *Sharp*, 1973; *Malin and Dzurisin*, 1977; *Malin*, 1992; *Schenk and Bulmer*, 1998; *Moore et al.*, 1999; *Chuang and Greeley*, 2000]. The character of extraterrestrial movements can only be inferred from the resulting deposits’ morphologies since resolution is nearly always insufficient to observe individual particles within the deposits.

With few exceptions, details of slope modification on Io generally are not obvious in Voyager images. Voyager 1 images of Io revealed steep slopes on the flanks of isolated mountains, along interior walls of calderas, and as scarps within plains units. *McCauley et al.* [1979] and *Schaber* [1982] reported observations of arcuate or digitate scarps, especially those in the south polar region, that suggested that some slopes on Io were subject to recession by mass wasting. *Schaber* [1982] reported lobate scarps along the flanks of some mountains which he noted resembled large landslides. *Schenk and Bulmer* [1998] recognized and discussed in detail a large debris apron along the southernmost flank of Euboea Montes, evaluated, in part, from a stereo-derived topography model. *Schaber* [1982] observed the absence of slumps in caldera walls and proposed that this was strong evidence for substantial wall strength.

In most cases, Galileo images acquired at ≤ 200 m pixel⁻¹ resolution and high incidence angle and/or in stereo were required to reveal landforms on icy Galilean satellites characteristic of mass movement [e.g., *Moore et al.*, 1999; *Chuang and Greeley*, 2000]. This is also true for Io. Here we report observations made during the first three close Galileo flybys (I24, I25, and I27) of that satellite, which took place in late 1999 and early 2000. In this study we identify and describe

¹ NASA Ames Research Center, Moffett Field, California.

² Center for Radiophysics and Space Research, Cornell University, Ithaca, New York.

³ Department of Geological Sciences, Arizona State University, Tempe, Arizona.

⁴ Department of Geological Sciences, Brown University, Providence, Rhode Island.

⁵ Lunar and Planetary Laboratory, University of Arizona, Tucson, Arizona.

⁶ Now at Astrophysical and Planetary Sciences Department, University of Colorado, Boulder, Colorado.

⁷ Lunar and Planetary Institute, Houston, Texas.



Figure 1. A mosaic of the Tvashtar caldera complex (centered at $\sim 60^\circ\text{N}$, 120°W) shows four volcanic vents in this area, one of which was erupting during the I25 flyby, creating the pixel bleed seen on the image. Three of the four vents are distributed across the floor of the depression that, in turn, is partly enclosed within a plateau rising ~ 1 km above the surrounding plains. Along scarps of this plateau several different slope types are seen. Boxes indicate the locations of subsequent figures used to illustrate individual slope types (numbered by figure). The letter “A” marks the location of alcove-rimmed canyons discussed in the text. (Mosaic is composed of images 251C040 and 251I0041 with nominal resolutions of 183 m pixel^{-1} , superposed on a portion of a 1.3 km pixel^{-1} , global mosaic acquired during orbit C21. The view is oblique. Illumination is from the left. North is up.)

slope morphologies seen in the new images of Io that are indicative of slope degradation and mass wasting and develop working hypotheses for the processes and materials involved in the evolution of these landforms.

2. Observations and Interpretations

The I24, I25, and I27 Io observations show several distinct degradation styles of slopes associated with mountain sides, caldera walls, and plateau margins, but degradational style does not always correlate directly with tectonic or volcanological setting. We begin with the rich variety of slope morphologies in the area of Tvashtar Catena ($\sim 63^\circ\text{N}$, 123°W) seen in observations 25ISGIANTS01 and 27ISTVASHT01 (which also provide stereo information), then turn to other Galileo observations elsewhere on Io where similar slope morphologies are found. Finally, we discuss two very high resolution observations that, while very selective in coverage, offer additional insights into slope degradation on Io.

The I25 mosaic of the Tvashtar caldera complex (Figure 1) shows four recently active volcanic vents in this area, one of

which was erupting during the I25 flyby [McEwen *et al.*, 2000]. Three of the four vents are distributed across the floor of a 70×170 km depression that, in turn, is partly enclosed within a plateau rising about a kilometer above the surrounding plains [McEwen *et al.*, 2000; Turtle *et al.*, this issue]. Four distinct slope morphologic types are found along the caldera walls and the extensive inward and outward facing walls of the plateau margins. These morphologies, described in detail below, reflect four different styles or states of slope degradation and may also reflect variations in material strength and/or susceptibility to modification processes. These morphologies also are seen elsewhere on the planet in other Galileo observations.

2.1. Type U Slopes

The southeastern vent of the Tvashtar complex is a kidney-shaped pit with a flat floor spanning about 30×60 km (Figure 2). The steep walls lining this pit generally lack deep alcoves or alternating spurs and gullies. Consistent with interpretations of similar pits by many previous workers, this pit proba-

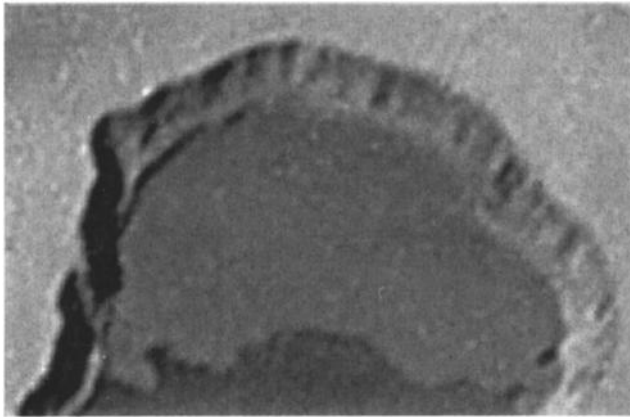


Figure 2. Type U (unmodified) slopes exhibit steep, unmodified walls lining a caldera, generally lacking significant modification. Width is ~ 30 km. View is oblique.

bly is a collapse caldera [Radebaugh *et al.*, this issue]. A low internal ledge runs continuously around the caldera floor. This ledge forms a steep, short cliff, so it probably represents material from a former, higher level of the caldera floor, rather than accumulations of disaggregated debris mass-wasted from higher exposures on the walls. We characterize type U slopes as relatively steep, with poorly developed alcoves, spurs, and gullies. A basal ledge may be present as in the current example from the southeastern caldera at Tvashtar, or any number of initial morphological variations present, but the important distinction is that the collective characteristics of type U slopes provide no convincing evidence of significant degradation beyond minor spur and gully modification and are largely unmodified by mass wasting at the observed scale.

2.2. Type D Slopes

Outward facing slopes along the western margin of the plateau at Tvashtar consist of cliff-forming walls above a less steep slope component that descends to the surrounding plains (Figure 3). The characteristic two-component slope profile, including the proportion of cliff exposure to the subjacent, less steep unit and respective gradients of each, appears relatively uniform along the slope, but resolution limitations and compression and radiation artifacts in the images limit quantitative determinations [Klaasen *et al.*, 1999]. The transverse profile along the scarp brink is irregular but is not dominated either by convex- or concave-out segments.

The overall slope configuration appears consistent with debris accumulating as talus immediately below the cliff-forming material, presumably produced by numerous relatively small mass-wasting events each involving release of minor amounts of material from the upper, cliff-forming exposures. Cliff faces still compose about half the slope relief, and this, combined with the poorly developed alcoving revealed along the transverse brink profile, suggests that the scarp may have receded only slightly from its original position. However, these estimates are complicated by the possibility that not all disaggregated material (and not all of the original relief of the slope) remains in view. Additional debris may be buried to unknown depth by later volcanic materials deposited on the surrounding plains, or some portion of the debris volume might have been transported away.

The gradient of the lower slope component appears relatively consistent, but this has not been confirmed quantitatively to be within the range of likely angles of repose for particulate materials. Even if this could be verified, a Richter slope [Bakker and Le Heux, 1952; see also Selby, 1993, Plate 16.2], in which only a thin veneer of debris covers a sloping rock core, could be present. Most debris weathered from a Richter slope would have to be transported elsewhere, however, or possibly buried and hidden at the slope foot by volcanic materials. While these possibilities cannot be ruled out, there is, again, no evidence for substantial burial of the slope since it formed or for a transport mechanism to carry away debris. Similar difficulties and uncertainties apply to another alternative in which the cliff-forming unit could represent a resistant caprock layer protecting a lower, more friable unit revealed by its lower gradient. In this scenario, the lower slope component is not primarily debris but a sloping rock face subject to degradation and debris removal, possibly causing minor undercutting of the upper, more resistant unit in the process. No evidence for undercutting of the upper unit can be resolved along the break in slope where these two units meet.

In summary, type D slopes, as seen along the western edge of the plateau at Tvashtar, have consistent slope profiles that are characterized by a steep, cliff-forming member overlying a shallower gradient slope component. The lower, less steep component is probably dominated by debris derived from many individual small releases of material disaggregated from the cliff-forming member directly above. The lack of deep alcoving along the scarp brink suggests that disaggregation rarely involves large releases of material that would substantially affect the transverse profile.

2.3. Type A Slopes

Slopes in the eastern and southeastern portions of the plateau at Tvashtar have sharp brinks and are deeply and con-

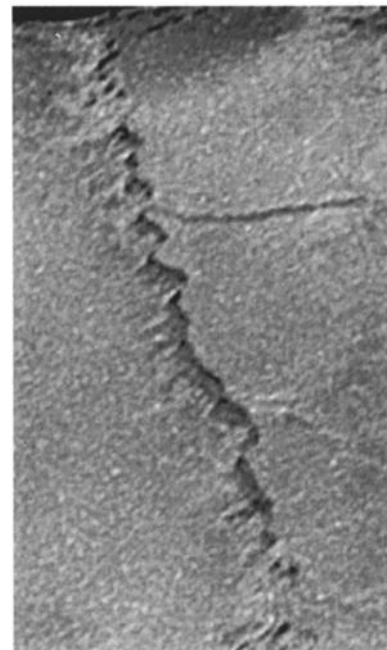


Figure 3. Type D (debris) slopes consist of cliff-forming walls above a less-steep component that descends to the surrounding plains (left). Width is ~ 35 km. View is oblique.

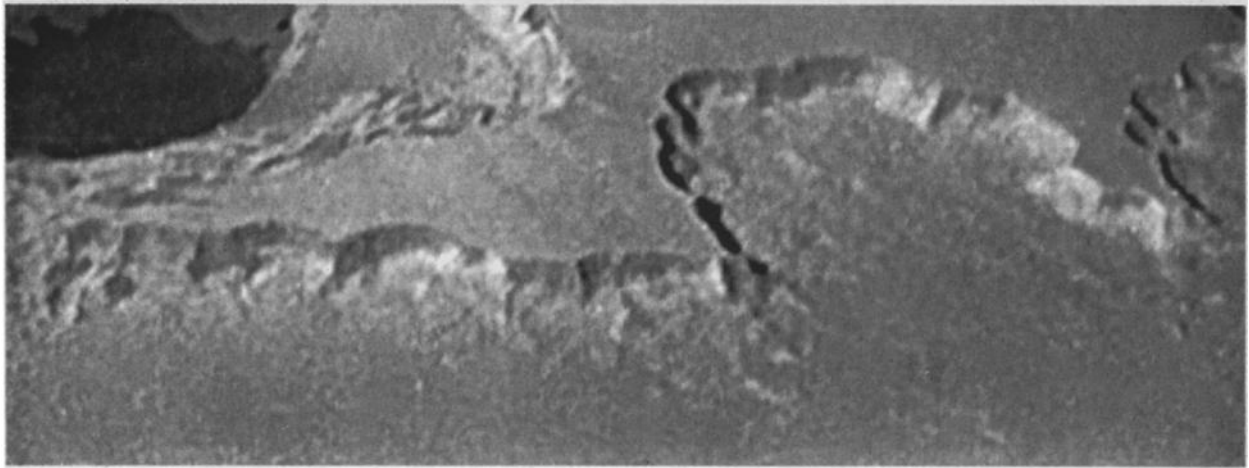


Figure 4. Type A (alcove) slopes have sharp brinks and are deeply and consistently scalloped, forming a series of adjacent alcoves. Gradients become less steep at lower elevations to form concave-up slope profiles. The lower portions of these slopes are more concave, longer, and rougher than the (straighter, shorter, and steeper) lower components of type D slopes. In many instances the hummocky materials in the lower portions of each alcove extend outward as irregular lobes with very low relief. Width is ~ 90 km. View is oblique.

sistently scalloped, forming a series of adjacent alcoves. Gradients become less steep at lower elevations to form concave-up slope profiles (Figure 4). Headwalls of the alcoves appear featureless at available resolution, but slopes become rougher at lower elevations where gradients decrease and merge onto the surrounding plains. The lower portions of these slopes are more concave, longer, and rougher than the (straighter, shorter, and steeper) lower components of type D slopes. In many instances the hummocky materials in the lower portions of each alcove extend outward as irregular lobes with very low relief, suggesting these materials originated from the alcoves and moved down and laterally away. These hummocky lobes typically extend of the order of an alcove width out onto the surrounding plains, but in many cases the terminations of these lobes out on the plains cannot be reliably recognized among or distinguished from other scattered low-relief hummocks and small, very low mesas that all have margins and relief similar to the low-relief lobes extending from the alcoves.

Type A slope morphology is consistent with scarp recession involving fewer, larger individual mass movements than for type D slopes, as suggested by the sizes of the alcoves and the volumes of material in the lobes extending from them. It is unclear if a volume discrepancy exists between the alcoves and hummocky materials within and extending from them. For this reason, it is difficult to be certain how far these slopes have receded. Crude estimations that restore all hummocky material to fill the alcoves and reconstruct the prior slope topography suggest slopes have receded distances similar to their overall height (slightly further, relatively, than type D slopes).

However, type A slopes also occur along the walls of several canyons that penetrate up to 40 km into the eastern part of the plateau, and it is possible that the mechanism for removing the material from these canyons is the same as or closely related to slope processes producing their alcoved walls. In this scenario some mechanism (such as sapping) erodes the base of the walls, removing material from the slope face (partially by undermining), and evacuating the overlying debris.

Despite morphological hints that sapping could be involved, there are no direct indications of fluid flow on the canyon floors or of reservoirs away from the canyons where canyon material might have been deposited. Such features could have been buried by younger volcanic materials on the canyon floors and elsewhere or simply be too subtle to be recognized in the images.

For instance, it is possible that the canyon floors resemble the surrounding plains as well as plateau surfaces simply because the canyons formed tectonically from these surfaces rather than erosionally. The origin of a large, ~30-km alcove system opening to the south from the southeastern corner of the plateau at Tvashtar (Figure 4, right) could be due to particularly active erosion and transportation (e.g., by sapping or plastic ice deformation with subtle relief on the floor of this alcove system representing a low-relief remnant debris field). However, in support of a tectonic hypothesis it is notable that the four largest calderas of the Tvashtar system are distributed along a southeastward trend, suggesting tectonic control (Figure 1). The large alcove system opening of the southeastern Tvashtar plateau is located along this trend, suggesting that this alcove system is in a likely place for a structural depression of this size to occur. Furthermore, the subtle low relief on the floor of the alcove system is morphologically identical to various expressions of low-relief plains elsewhere in the area that have no demonstrated relationship to slope processes. A tectonic hypothesis implies much less back wasting than the erosional hypothesis. Uncertainty on this issue implies uncertainty in estimations for recession of type A slopes on Io. Without further evidence, it remains ambiguous whether type A slopes indicate only local recession with total volumes related closely to current alcove geometry or indicate much greater amounts of recession involving the transportation of correspondingly larger volumes of material significant distances away from the slope.

Hummocky materials in the lower portions of each alcove extending outward as irregular, low-relief lobes could simply be landslide deposits. An alternative emplacement mechanism is solid-state creep. This speculative solid-state mecha-

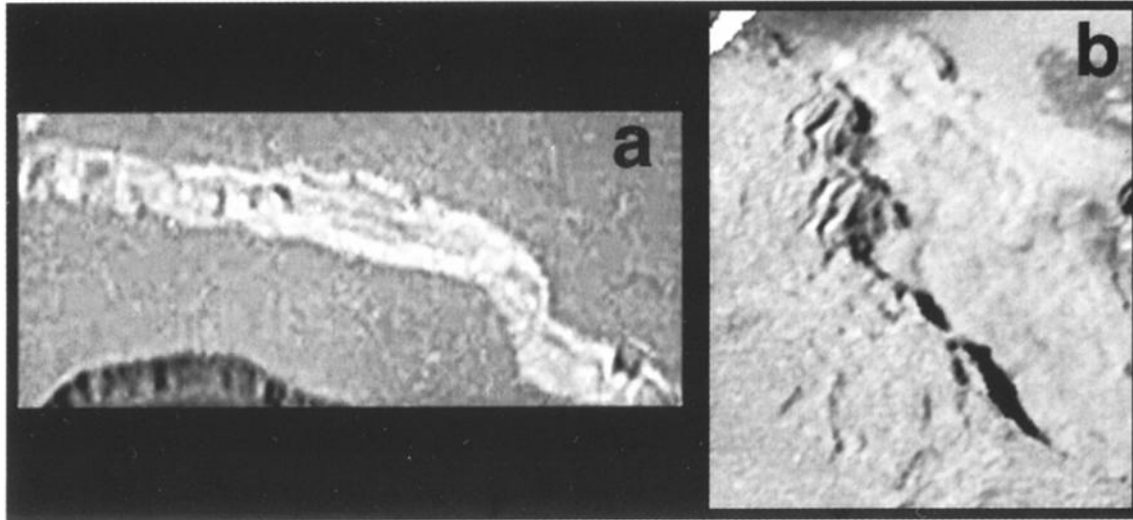


Figure 5. Type T (terraced) slopes are characterized by subparallel terracing at higher elevations and (in most cases) hummocky material ending at distinct, sometimes convex-up, lobate margins at lower elevations. (a) Prominent terracing along the scarp face. (b) Less face terracing but small prominent parallel scarps behind the main scarp. Figure 5a is ~ 55 km wide, and Figure 5b is ~35 km wide. The view is oblique.

nism might involve contributions from a ballistically emplaced volatile component in pyroclastic deposits, which, after accumulating on slopes to a threshold thickness, could enable movement of the entire deposit, including debris shed from the slope itself, downslope under its own weight, analogous in some ways to water-ice-cored active rock glaciers on Earth. This process will be considered in more detail in section 3.4.

2.4. Type T Slopes

Type T slopes are characterized by subparallel terracing at higher elevations and (in most cases) hummocky material ending at distinct, sometimes convex-up, lobate margins at lower elevations but there are wide variations within this category. Type T slopes at Tvashtar are most prominent along the southern-to-western inward facing walls of the plateau, and along the southwestern outward-facing walls (Figure 5a). Less prominent examples are found along eastern inward facing plateau walls (Figure 5b). The relative size of the lower hummocky component varies considerably with location and seems correlated with the degree of terracing. The hummocky unit extends up to 20 km from the western inward facing walls where terracing is most developed, extends <10 km from the southern inward facing walls and is not found at all along the foot of the eastern inward facing wall. In the latter case, where terracing is also much less prominent, the lower hummocky unit may have been much smaller or lower to begin with, then was buried by volcanic materials from the adjacent calderas. Burial might also truncate the exposures of other hummocky deposits elsewhere around the walls rimming the large 70 x 170 km depression. Along the southwestern outward facing walls, the hummocky component with convex-up margins is so prominent that it composes more of the total slope relief than the subparallel terracing farther up-slope.

Type T slope morphology is consistent with brittle failure, coherent slumping, and in some instances partial rotation of

slope walls, producing terraces and minor scarps near the head of the failure surface. Slope material is transported down and laterally away to form hummocky deposits with margins that are resolved as convex-up in the largest cases. Subparallel terracing on type T slopes is the most consistent morphological distinction from type A slopes (which are marked by alcoves at their higher elevations) and indicates a different mass-wasting style. Multiple terracing of type T slopes suggests that slope recession in these locations is a progressive process involving many separate large failures.

In contrast, there are no indications of even minor terracing behind the alcoves of type A scarps, suggesting that alcove-creating slope failures are singular events or at least much smaller and/or rarer. This could mean that destabilizing effects such as removal of toe material or raising of relief (e.g., by lowering the base level) occur more frequently along type T slopes. If so, this would be consistent with most type T slopes at Tvashtar occurring along inward facing plateau margins, where the base level might be subject to fluctuations from activity in the magma chamber system beneath the calderas. The series of failures creating the type T slope along the southwestern outward facing margin is harder to understand. The hummocky run-out deposit here is especially prominent, and subparallel terracing occurs as much as 50 km back from the slope margin. Portions of the plateau appear to have broken up in response to lateral tensional stresses, with uplift of the plateau margin as a possible stress source.

2.5. Slope Exposures at Other Localities

Many slopes on Io have morphologies similar to the four slope types described above in the Tvashtar area. Type A slopes, variations of type T slopes, and perhaps type U slopes are found along plateau margins and mountain sides seen in the Zal Montes and its surroundings (251STERM01 and 271SZALTRM01 Galileo observations). The Zal Montes (Figure 6) consist of a 60 x 150 km plateau and a higher-relief complex ridge trending SSE for 200 km [*Turtle et al.*, this is-

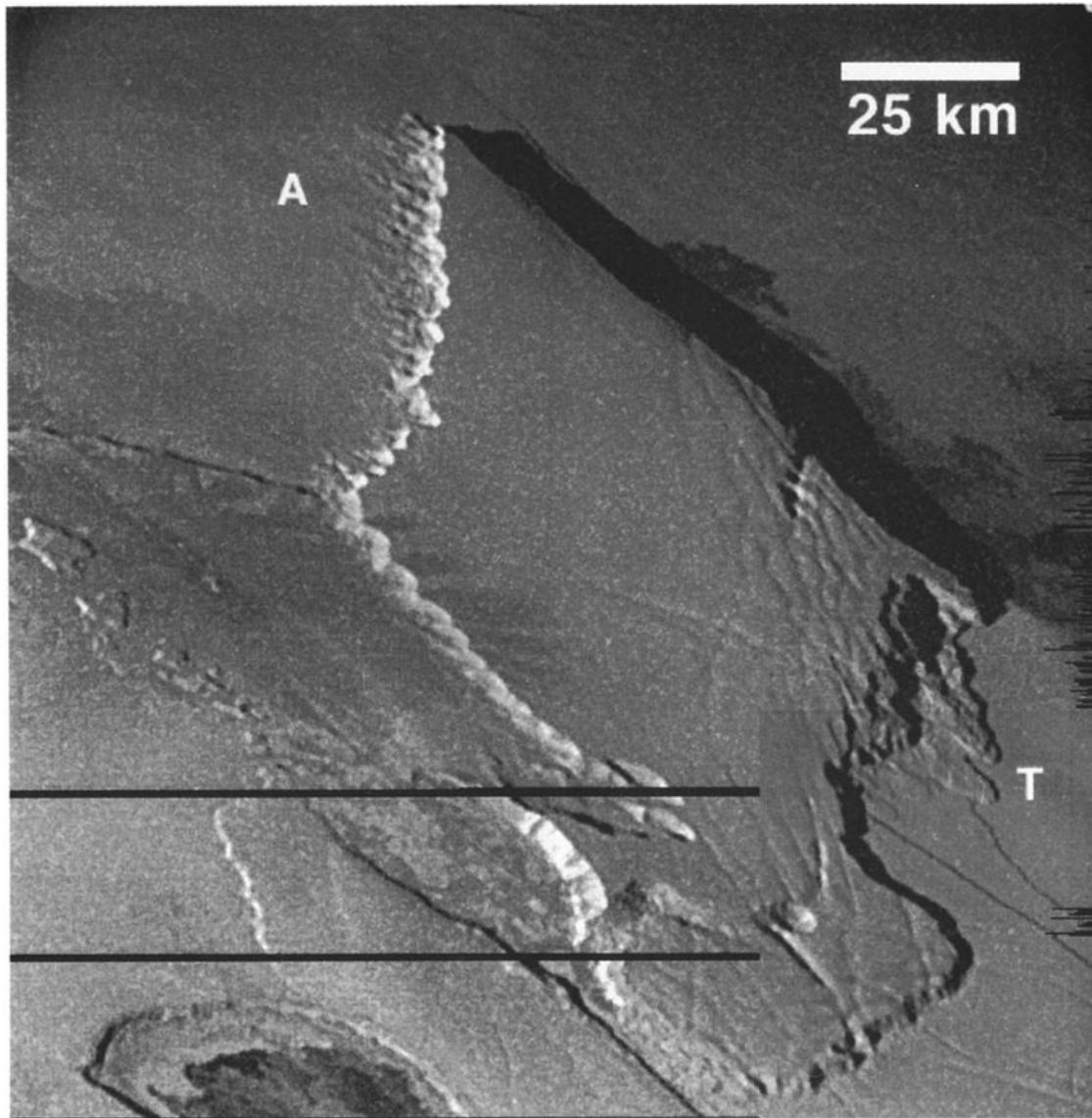


Figure 6. A plateau in the Zal Montes located at $\sim 42^{\circ}\text{N}$, 77°W exhibiting two types of slopes (images 2510060 and 2510061, 260 m pixel^{-1}). Type A slopes are found near “A,” and type T slopes are located near “T.” The view is oblique. Illumination is from the left. North is toward the top left.

sue]. A 120-km-diameter caldera lies between these constructs. The area is seen closer to the terminator in the 260 m pixel^{-1} I25 observation, which also includes an isolated unnamed mountain to the southwest, but the 335 m pixel^{-1} I27 observation (Figure 7) has more complete coverage of the higher-relief SSE trending mountain ridge. Type A slopes are prominently displayed along the northern margin of the plateau; the viewing geometry shows characteristic lobate deposits extending up to 30 km from individual alcoves (Figure 6). Subtle albedo patterns on the plains beyond the lobate deposits could mark where fluid-like material has flowed from the type A slopes. However, these patterns also are very similar to those commonly found elsewhere on plains far from slopes and so may simply be lava flows. Shallow troughs and swales on the southeastern part of the plateau transform near the southern margin into terraces of type T slopes. Hummocky lobes (thicker and more extensive than those associ-

ated with type A slope alcoves on the other side of the plateau) extend 40 km to the south from these terraced scarps.

Subtle near-horizontal lineations mark west facing slopes of the northern end of the higher-relief mountain ridge in the Zal Montes (Figure 7). These could represent remnants of layered plains material uplifted with the main mountain mass [Schenk and Bulmer, 1998; Turtle *et al.*, this issue]. Alternatively, these features could mark the locations of slump terraces typical of type T slope degradation. For this scenario we speculate that the massif progressively shed relatively weaker near-surface materials aside during uplift as it emerged at the surface; the original surface materials progressively shoved aside by the steep, emerging massif peak are the terraced, lower gradient materials composing the lower portion of the mountainside. Extended hummocky run-out deposits are absent from the plains at the foot of this slope, but there are two possible explanations: (1) slumping materials simply may not

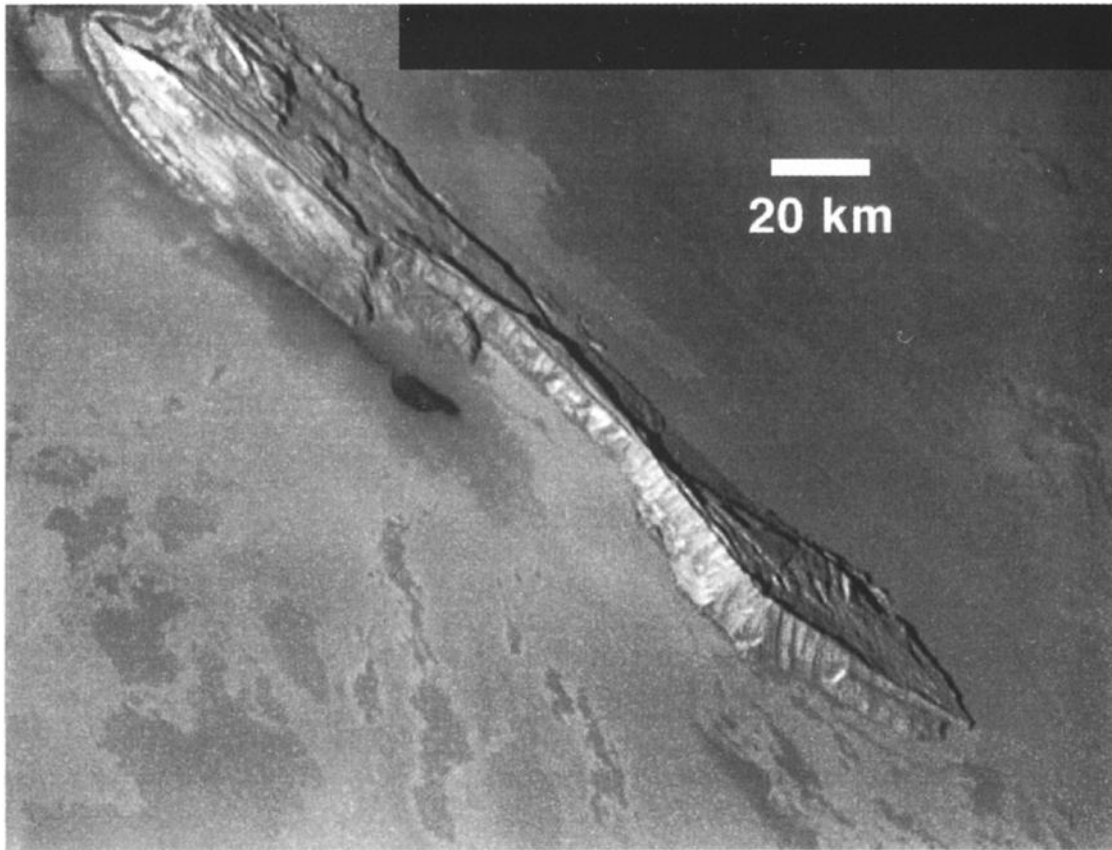


Figure 7. A ridge in the Zal Montes located at $\sim 35^{\circ}\text{N}$, 73°W . Note the subtle near-horizontal lineations mark west facing slopes of the northern end of the higher-relief mountain ridge, which could mark the locations of slump terraces typical of type T slope degradation (images 2710059 and 2710060, 335 m pixel^{-1}). The view is oblique. Illumination is from the bottom left. North is toward the top left.

have been shoved laterally very far as the massif emerged at the surface and/or (2) longer run-out landslide deposits may have been generated either during massif uplift or later degradation of the slope but they may have been covered or eroded away by subsequent volcanic eruptions (e.g., by lava flowing north along the foot of the slope from a small adjacent caldera).

Two mountain complexes associated with Gish Bar Patera are captured in the eastern half of the $480\text{-}570\text{ m pixel}^{-1}$ 24ISAMSKG101 observation (Figure 8). Variations of type T slope degradation are found on all of these features. A plateau extends westward from the larger mountain complex near Gish Bar Patera. This plateau has a lobate, digitate western margin that may be a landslide deposit. As discussed previously for the smaller isolated mountain to the northeast, an alternative hypothesis for this type of morphology involves massif uplift disturbing a much weaker overlying surface layer where the massif emerges from the surface. The alternative explanation was also explored by *Schenk and Bulmer* [1998] for a feature associated with the Euboea Montes. Continued uplift results in the weaker surface materials being partly raised and partly compressed laterally as they are gradually shed aside. This process produces relatively high-relief mountain slopes with two elements: a steeper, upper component corresponding to the massif itself (probably with a minimum of adhered debris from originally overlying surface

materials); and a lower, less steep component consisting of a series of partly compressed, tilted, and potentially unstable slumps of what were originally surface deposits, covering the lower flanks of the uplifted massif and extending outward along the surrounding plains. Few details are exposed on the slab-like, almost featureless upper flanks of this mountain complex, similar to the upper flanks of the smaller isolated mountain to the northeast. Skythia Mons is a more extended, lower-relief structure than the mountains around Gish Bar Patera. The flanks of Skythia Mons display alternating grooves and ridges oriented only approximately perpendicular to local gradient (Figure 9). Minor examples of these striations along the eastern lower flanks might owe part of their character to expressions of internal layering, but elsewhere, especially along the southeast margin, this texture does not convincingly suggest exposures of horizontal strata. Instead, the striations along the southeast margin define arcuate (concave outward) patterns that are expressed at lower elevations as a series of shallow alcoved terraces with arcuate scarps. Perhaps structural disturbances are largely responsible for the striated relief around the margin of this prominent plateau, and along the southeast margin these disturbances have caused back wasting of the plateau by slumping of the flanks.

The margins of Shamshu Mons (Figure 10), imaged at 342 m pixel^{-1} during I27, show evidence of type A slope degradation but with morphological variations perhaps linked to ob-



Figure 8. The mountain complex near Gish Bar Patera (images 2410111 and 2410117, $\sim 500 \text{ m pixel}^{-1}$). The plateau at left has a lobate, digitate western margin interpreted as a landslide deposit. The view is oblique. Illumination is from the left. North is roughly up.

scuration by lava flows. Unlike type A slopes in many other places, alcoves along the northwest facing flank of Shamshu Mons have flat floors with no traces of low-relief lobes extending from them. Lava apparently has flowed northeast from a small caldera into the trough between the alcoves and an outlying, parallel ridge, burying the lower portions of the alcoves and forming their flat floors.

Very high resolution images with resolutions $< 10 \text{ m pixel}^{-1}$ were also obtained by Galileo, but these images cover an extremely small portion of the satellite so their content is almost certainly not truly representative of the entire surface or processes that occur there. Nevertheless, these images begin to show more of the actual geological complexity of the surface than more widespread, lower-resolution images can. Chaac caldera scarp (Figure 11) is captured in two images of the $\sim 9 \text{ m pixel}^{-1}$ 27ISCHAAC_01 observation. Most of the scarp length captured in the images consists of a very steep cliff-forming member extending from a sharp brink at the plateau edge right down to the caldera floor; shadow measurements indicate this cliff-forming member has a total relief of 2.8 km and descends at a gradient of around 70° [Radebaugh *et al.*, this issue]. The walls are dimly lit by scattered light in

shadow. The cliffs appear massive, with few hints of layering or of gullies or other features consistent with mass wasting. At lower resolution this would probably be identified as a type U (largely unmodified) slope. In some places, cliffs descend only about three fourths of the way to the caldera floor before changing abruptly to a component with a much lower gradient that descends the remainder of the total relief of the slope. The relatively consistent gradient of this lower component suggests that it could be debris accumulated from many small releases from cliff-forming material immediately above. However, several details suggest that an explanation as talus might be too simplistic. The interpretation of the lower-component material as talus would be more secure if there were corresponding cavities or gullies immediately above to suggest where this volume of material originated, but the scarp brinks appear as continuous in these locations as elsewhere along the walls where cliffs extend all the way down to the caldera floor. In one area the putative talus has an albedo pattern that cannot be explained easily as a shadows from the cliffs above but might be consistent with fingers of dark talus slumping down older, brighter exposures of the same unit in minor stability adjustments. It is not clear why at some point in the past portions of this putative talus would have been brighter, but complications associated with caldera activity could be involved. There are bright patches immediately adjacent on the caldera floor, and whatever brightened this portion of the caldera floor might also have brightened the putative talus unit at one time; subsequent releases from the cliff-forming unit would be darker and would gradually cover bright deposits on the talus beginning at the higher elevations immediately below the cliffs.

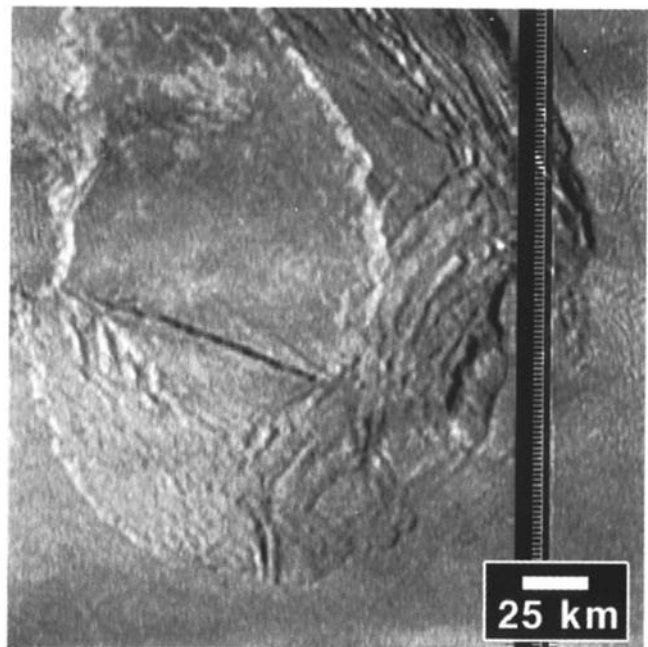


Figure 9. Striations along the southeast margin of Skythia Mons ($\sim 26^\circ \text{N}$, 97°W) define arcuate (concave outward) patterns that are expressed at lower elevations as a series of shallow alcoved terraces with arcuate scarps, which may be the result of back wasting of the plateau by slumping of the flanks (image 2410110, $\sim 500 \text{ m pixel}^{-1}$). The view is oblique. Illumination is from the left. North is roughly up.

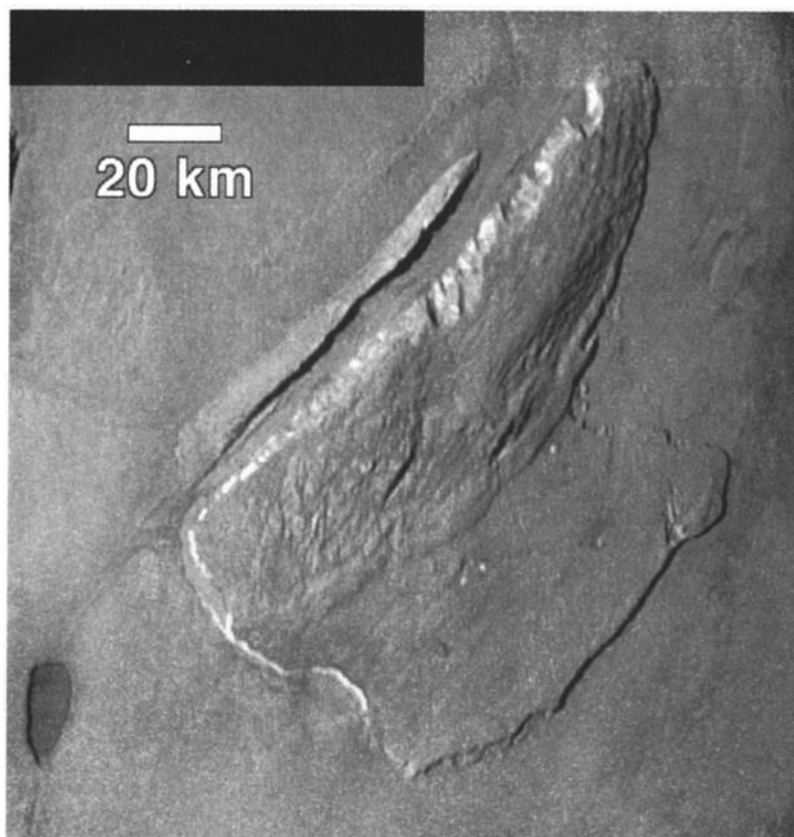


Figure 10. Margins of Shamsu Mons ($\sim 12^{\circ}\text{S}$, 72°W), show evidence of type A slope degradation but with morphological variations caused by the lower portions of these slopes being obscured by lava flows (images 2710065 & 2710066, 342 m pixel^{-1}). The view is oblique. Illumination is from the upper left. North is toward the upper right.

Ridge sets seen on some mountain flanks, such as Hi'iaka Montes (Figure 12), appear interleaved or en echelon. Ridges bifurcate in some cases and have convex to convex-ramp terminations. Ridges in cross-trend profile appear rounded and may be the surface expression of folds. The morphology of individual ridges and the arrangement of ridge sets might best be interpreted as the manifestation of compressional folds in a surface layer overlying a shallow decollement, or perhaps a ductile subsurface [Pappalardo and Greeley, 1995]. This ridge texture is most pronounced on slopes, which suggests that they formed by gravity sliding of a detached surface layer. The orientation of ridges is always perpendicular to gradient where this texture is found. If Io's mountains form by the tilting of preexisting crustal blocks, the shallower ridged facet may be the original (formerly flat) premountain surface. Cumulative successions of plume fallout, SO_2 condensates, landslide material, and lava flows probably form stacks of thin, areally extensive layers within the plains. If such stacks of material have weak layer-to-layer contacts, they would be susceptible to deformation and detachment when tilted. Schenk and Bulmer [1998] proposed a similar configuration as a contributor to mountain landslides on Io.

Figure 13 shows one image from an 11-image observation of a very small portion of Ot Mons obtained at very high resolution (9 m pixel^{-1}) and low sun that we interpreted as a close-up view of ridge texture on mountain flanks such as is shown in Figure 12. Pre-encounter pointing predicted that

Figure 13 is located on the north flank of Ot Mons, but unfortunately, the best available lower resolution context is a $\sim 2\text{ km pixel}^{-1}$ image acquired during the E14 encounter (Figure 14). In the high-resolution images the surface is covered by E-W trending ridges $\sim 1\text{-}2\text{ km}$ long and $0.25\text{-}0.5\text{ km}$ wide. Just as with the ridges seen elsewhere at lower resolution (e.g., Figure 12), the Ot Mons ridges exhibit pinches and swells. Unlike the ridges in Figure 12, some of the Ot ridges appeared breached or disrupted. These breaches or disruptions take the form of steep-walled amphitheatres. These amphitheatres are often elongate and trend the same direction as the ridges. The floors of the amphitheatres are often covered with dark material that might have moved downslope to accumulate there. Terracing within the walls of the amphitheatres might be layering exposed by the amphitheater-forming process. If the Ot Mons flank ridges are indeed anticlinal ridges, such ridges commonly have extensional features along their crests [Pappalardo and Greeley, 1995]. We speculate that the amphitheatres have formed initially as anticline crestal fractures and subsequently were widened into amphitheatres by an erosional process that involves the disaggregation of the outcrop.

During the I27 encounter, several 5.5 m pixel^{-1} images were acquired to look for evidence of layering and to investigate Io's erosional processes. These images show complex patterns with pronounced variations in texture and albedo (Figure 15). Further complicating the interpretations is the fact that

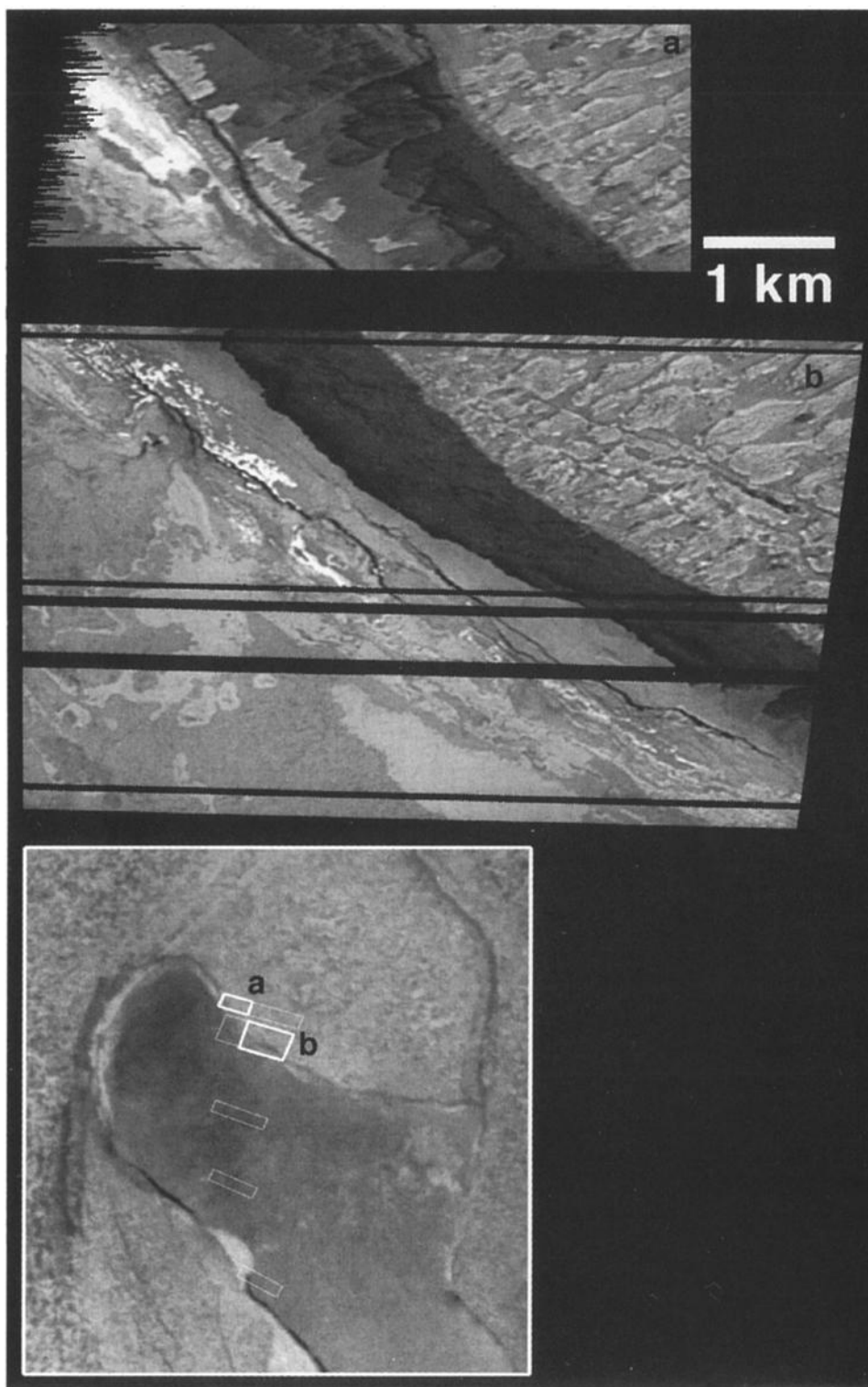


Figure 11. A portion of the Chaac caldera scarp illustrating a type U slope (top two images are located at $\sim 12^\circ\text{N}$, 158°W , images 2710009 and 2710010, $\sim 9 \text{ m pixel}^{-1}$). Most of the scarp length consists of a very steep cliff-forming member (mostly in shadow) extending from a sharp brink at the plateau edge (at right) down to the caldera floor (at left); shadow measurements indicate that this cliff-forming member has a total relief of 2.8 km and descends at a gradient of around 70° . The walls are dimly lit by scattered light in shadow, but the cliffs appear massive, with only few hints of layering, or of gullies or other features consistent with mass wasting. Illumination is high and from the right for the top two frames. The lower image (image 2710036, $\sim 180 \text{ m pixel}^{-1}$) provides context. The bold boxes locate the top two frames. Illumination is high and from the left for the context frame. North is roughly up.

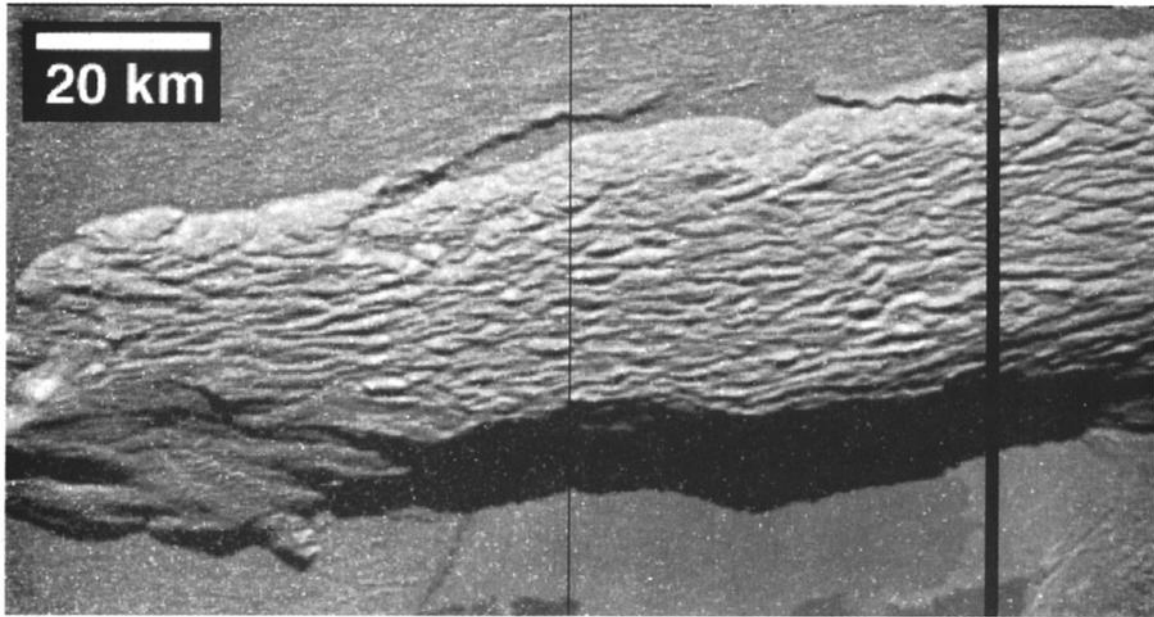


Figure 12. Ridge sets seen on some mountain flanks, such as here on one of the Hi'iaka Montes ($\sim 2^{\circ}\text{S}$, 83°W , image 2510064, 265 m pixel^{-1}), appear interleaved or en echelon. Ridges bifurcate in some cases and have convex to convex-ramp terminations. Ridges in cross-trend profile appear rounded and may be the surface expression of folds. Illumination is from the top. North is roughly to the right.

the images are quite oblique (60° - 70° emission angle). The scene shows a mesa or plateau scarp, largely facing away from the spacecraft, and the surface beyond the scarp's foot. Shadow measurements indicate the scarp exhibits $\sim 400\text{ m}$ of relief and a slope of $\sim 28^{\circ}$. There are hints of layering in the scarp face. A $\sim 1\text{-km}$ -wide belt or zone exhibiting bright and dark swirl patterns hugs the base of the scarp. The swirl belt's conformity to the scarp base can be interpreted to indicate that this material is being exposed by the retreat of the scarp. While only a small portion of the scarp is imaged, the portion visible is sinuous in plan form, unlike what would be

expected of a fault scarp. The swirl belt might be a lava flow along the base of the scarp, but generally, surfaces beyond scarp bases are usually highest near the scarp; thus lava flows generally would tend to not be scarp hugging. Farther out on the plain beyond the swirl belt, there appear to be small gullies cut into a blander, probably smoother surface, $10\text{-}20\text{ m}$ across and $100\text{-}200\text{ m}$ long, and roughly oriented perpendicular to the scarp (Figure 16). Beyond the gullied smoother belt is a thinner ($\sim 0.5\text{ km}$), darker, rougher belt or zone also apparently roughly paralleling the scarp trace (though image coverage is very limited). While this scene might be entirely

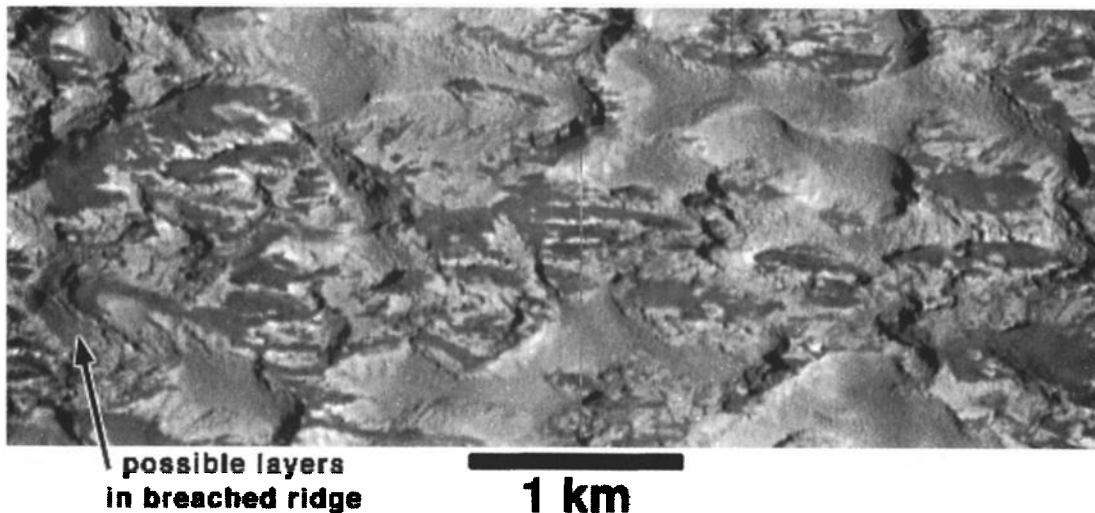


Figure 13. Very high resolution view of breached ridges on the north flank of Ot Mons ($\sim 4^{\circ}\text{N}$, 216°W , image 2410037, 9 m pixel^{-1}). The breaches take the form of steep-walled amphitheaters. Terracing within the walls of the amphitheaters might be layering exposed by the amphitheater-forming process. The view is near vertical. Illumination is from the left. North is down.

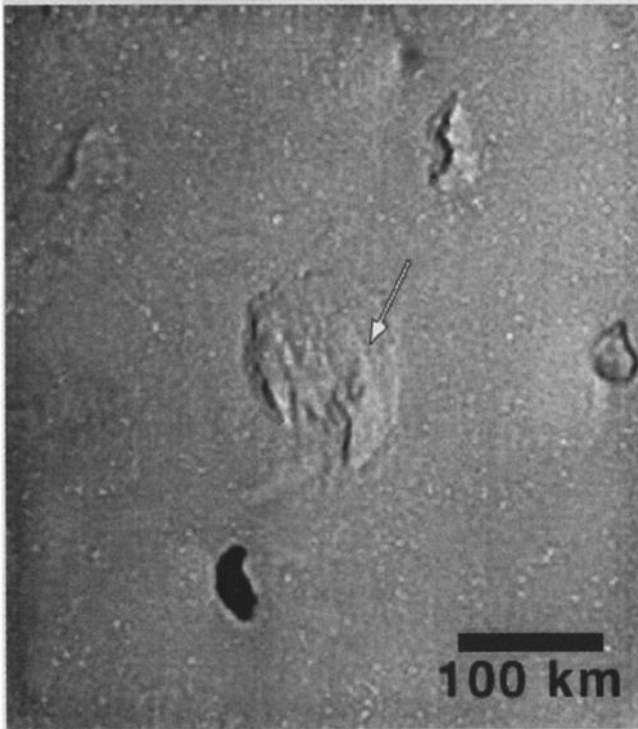


Figure 14. Preencounter pointing (arrow) prediction of the location of Figure 13 on the north flank of Ot Mons ($\sim 4^{\circ}\text{N}$, 215°W , image 14I0013). This best available context is a ~ 2.6 km pixel $^{-1}$ image acquired during the E14 encounter. Illumination is from the right. North is up.

the product of volcanism and tectonism, the series of seemingly circumferential belts or zones beyond the scarp and the plan trace of these features that we judge to imply a possible explanation involving the erosional retreat of the scarp, possibly involving the decay of relief-supporting material in the scarp face.

3. Discussion

Io shows clear and unambiguous evidence of downslope movement of material at a variety of scales and probably employing a variety of mechanisms. We now consider what may be producing these different landforms and surface textures. On Io, mass movements involving block release and brittle slope failure, as well as other processes such as sputtering, sublimation, sapping erosion from liquid SO_2 , the downslope movement of warm, plastically deforming SO_2 ice, and disaggregation from chemical decomposition of solid S_2O and other polysulfur oxides are candidate processes. We will next discuss these mechanisms in some detail.

3.1. Block Release and Brittle Slope Failure

Characteristic slope profiles of the four slope morphologies described in section 2 are summarized in Figure 17, along with the most likely (or at least the simplest, most readily supported) interpretations. Although processes such as sapping cannot be ruled out, we find no unambiguous evidence for liquid discharging at slope faces or debris transport requiring the presence of a liquid. Low-relief hummocky lobes extending from some slope faces could either be avalanche deposits or materials deposited from solid-state flow of a

volatile enriched debris, analogous to terrestrial water-ice-cored rock glaciers. Although observations appear consistent with mass wasting processes involving dry materials, it should be kept in mind that mass wasting involving fluids (e.g., debris flows, landslide deposits with long run-out distances lubricated by a fluid) could potentially involve thinly distributed volumes of relatively low relief that could be difficult to detect with available resolution. “Dry” mass movements involve slope materials that release in many small volumes or in fewer large volumes because of either a reduction in strength or a change in slope geometry (e.g., removal of slope toe by lowering of a caldera floor). Here the term dry is being applied using a well-known terrestrial mass movement classification scheme [e.g., see Coates, 1977; Malin, 1992, Figure 2] that compares material cohesion and particle size against speed of movement. This scheme groups mass movements requiring fluidizing lubrication (whether from air or water) to one extreme and those which require no lubricant (and hence are dry) at the other. Figure 17 shows how slope morphology changes as the size of the slope failure increases. Type D slopes result from the accumulation of many very small, block- or boulder-sized releases from cliff exposures. Larger, coherent failures of slope materials reaching more deeply behind the slope face create alcoves and type A morphology. Even larger slope failures result in the terracing seen in type T slopes.

In places such as Tvashtar all of these slope morphologies are present in relatively close proximity. How can this be explained? The inward facing slopes display three morphological styles: types U, A, and T. The outward facing slopes show two of the same morphologies, A and T, plus an additional style, type D, that is not seen on the interior walls. One possibility is that stronger materials are more abundant closer to the caldera than farther away. In this scenario the ratio of silicate lavas to more volatile-rich pyroclastic deposits decreases with increasing distance from the calderas, and silicate lavas might potentially produce steeper and more coherent linear scarps, while volatile-rich pyroclastic deposits might form potentially more unstable walls and encourage alcove formation. The contribution of this factor is difficult to assess or rule out with current data, but circumstantial evidence suggests that it is not necessarily the most important. A different scenario is that the four slope morphologies summarized in Figure 17 also define an evolutionary/time sequence, in which type U slopes are least evolved, followed by type D, and finally by either type A or T. Such a time sequence implies that steep slopes (1) are created as cliff-like scarps and (2) then progressively deteriorate as materials farther back behind the slope face are weakened somehow from proximity to the surface environment. In this scenario, slope degradational style is a function of age. Considering that volcanism at the calderas is certainly the high-frequency geologic activity in the Tvashtar area, it is not surprising that type U slopes are found closer to the calderas where renewal is most likely and that slope morphologies that might reflect greater exposure age and degradational development are further away. Outward facing slopes are less frequently disturbed so are left to more fully develop degradational morphologies.

3.2. Sputtering

The potential effect of magnetospheric sputtering increases substantially with decreasing distance from Jupiter. Hence Io should be most affected by this process. Sputtering at Io

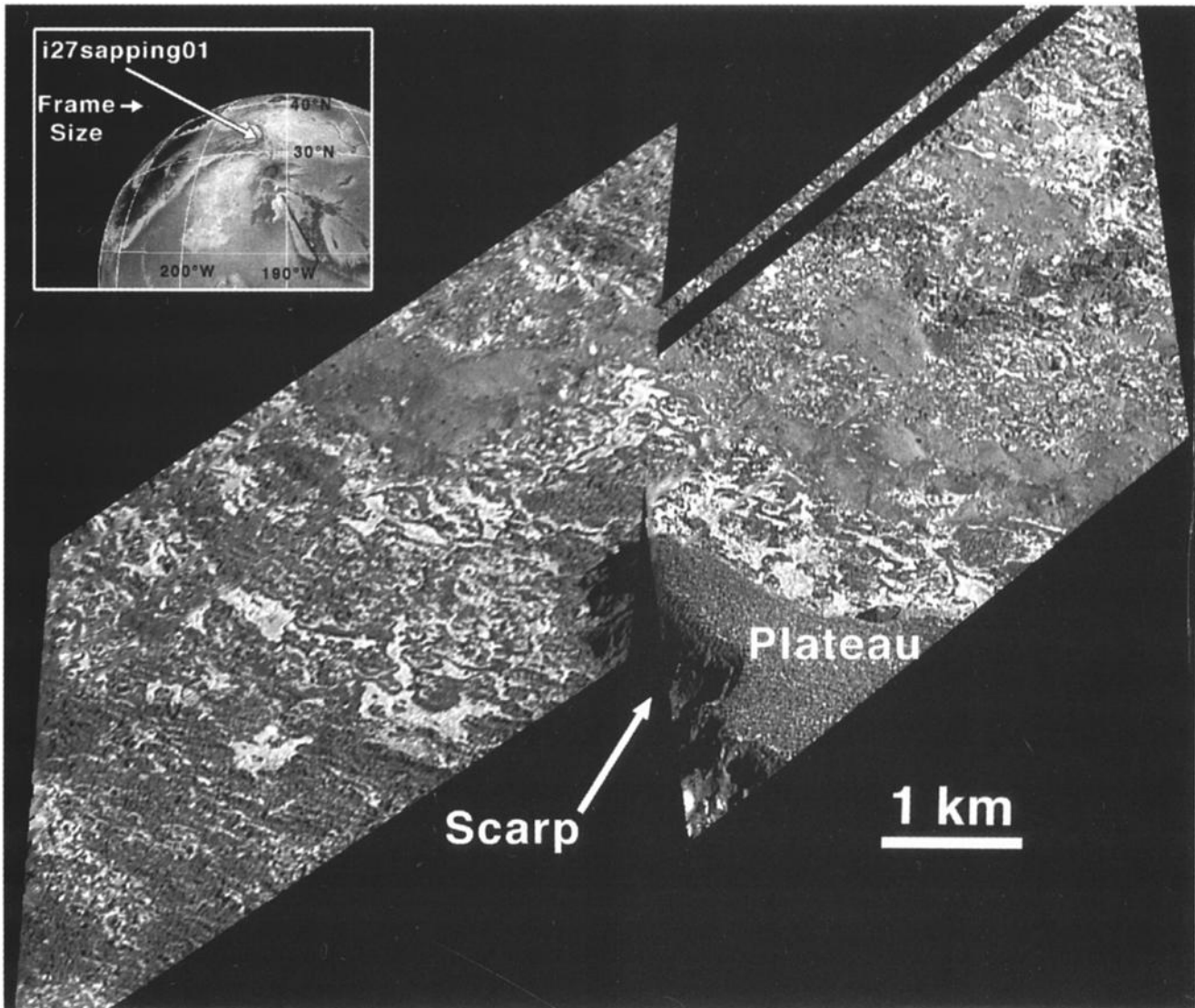


Figure 15. Very high resolution images (5.5 m pixel^{-1} , images 2710005 and 2710006) showing a mesa or plateau scarp, largely facing away from the spacecraft, and the surface beyond the scarp's foot ($\sim 32^\circ\text{N}$, 193°W , see context map at top left). Shadow measurements indicate the scarp exhibits $\sim 400 \text{ m}$ of relief and a slope of $\sim 28^\circ$. There are hints of layering in the scarp face. While this scene might be entirely the product of volcanism and tectonism, the series of seemingly circumferential belts or zones beyond the scarp and the plan trace of these features suggest the possibility that it could also be the consequence of erosional retreat of the scarp, possibly involving the decay of relief-supporting material in the scarp face. Original perspective highly oblique ($\sim 70^\circ$). Images reprojected to a common point perspective view similar to that from the spacecraft. Illumination is from the right. North is up.

would have a negligible erosional effect on silicates, such as basalt, and some effect on sulfur allotropes [Johnson, 1990]. Sputtering-induced erosion on Io would be most pronounced on exposures of unprotected SO_2 [Johnson, 1990]. As such, the amount of erosion of SO_2 due to sputtering over the age of Io's surface (generally accepted as not greater than $\sim 1 \text{ Myr}$ [e.g., Johnson and Soderblom, 1982]) determines the maximum erosion sputtering can cause on Io. Johnson [1990], in his summary of sputtering studies, gives a value of $5 \times 10^{11} \text{ molecules cm}^{-2} \text{ s}^{-1}$ for the maximum sputter erosion rate of SO_2 on Io. Over a million years this would result in a surface lowering of $\sim 1 \text{ m}$ for uncontaminated massive SO_2 ice ($\sim 1.5 \text{ g cm}^{-3}$) or $\sim 3 \text{ m}$ for uncontaminated porous SO_2 snow. Surface modification on this scale would probably be undetectable even in the highest resolution ($\sim 5 \text{ m pixel}^{-1}$) Galileo images of

Io. Thus other processes must dominate landform erosion observed by Galileo.

3.3. Sapping

A sapping mechanism involving liquid SO_2 was proposed by McCauley *et al.* [1979] to explain the irregular erosional scarps and bright deposits in layered terrains imaged by Voyager 1. Similar morphologies on Earth and Mars have been interpreted as due to the release of water to the surface combined with mass wasting [e.g., Carr, 1995]. Liquid water is highly unlikely on Io, but SO_2 will become liquid at some depth, depending on the isothermal gradient (probably highly variable in space and time). Artesian pressures would drive liquid SO_2 to escape through cracks, fissures, or permeable

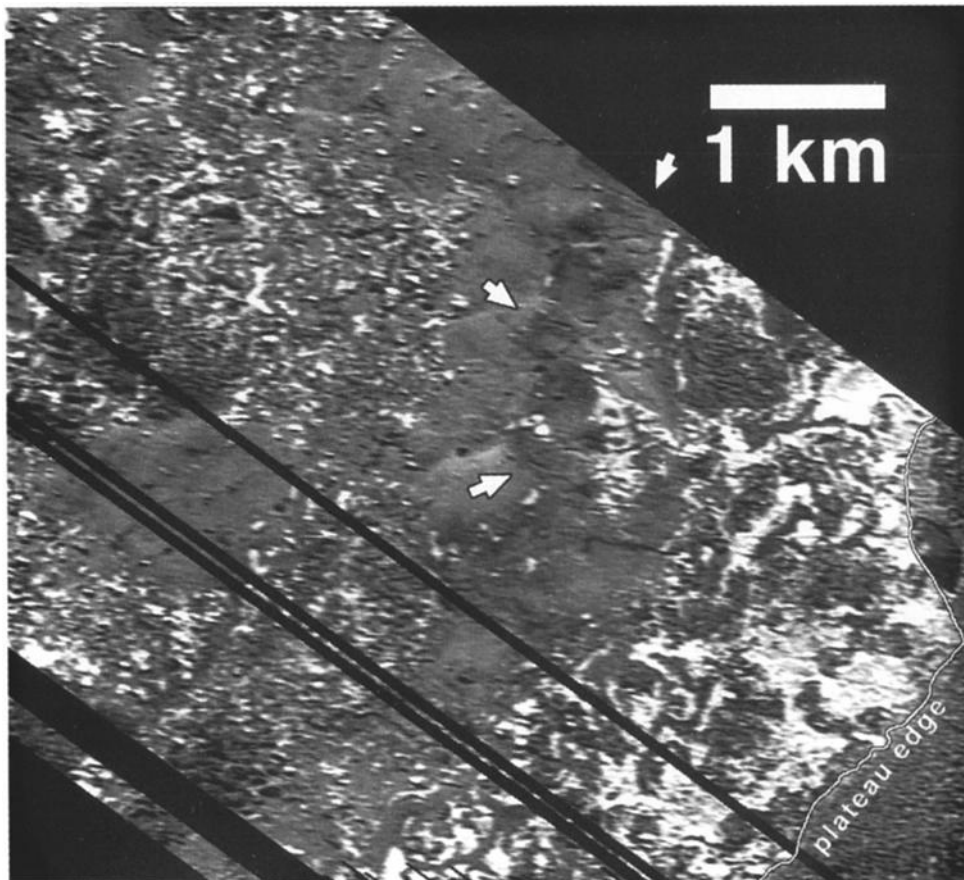


Figure 16. An orthographically projected excerpt from a portion of the right image (image 2710006) in Figure 15 showing what appear to be small gullies (see arrows) cutting into a blander, probably smoother surface. The gullies are 10-20 m across and 100-200 m long and are roughly oriented perpendicular to the scarp. Illumination is from above. North is to the left.

layers along the edges of scarps. The escape of SO_2 to the Ionian surface ($\sim 10^{-9}$ bar pressure) would cause vaporization, and an exit velocity of more than 350 m s^{-1} ; the SO_2 would snow back onto the surface up to 70 km from the vent. This is entirely consistent with the diffuse white deposits seen extending from the base of many irregular scarps on Io (see illustrations of *McCauley et al.* [1979]).

As discussed previously, deep alcoves into the plateau near Tvashtar Catena (Figure 1, see A) might have formed by sapping. Canyons $\sim 1 \text{ km}$ deep [*Turtle et al.*, this issue] extend up to 40 km into the plateau. The rectangular pattern of alcove-rimmed troughs in the Tvashtar plateau resembles “fretted” erosion along the highlands-lowlands boundary on Mars. The fretted morphology of this part of the Tvashtar plateau might be an example of liquid SO_2 exploiting and enlarging structural patterns of weakness (e.g., joints and fractures), causing disaggregation and further back wasting into the plateau. Sapping due to liquid water has been proposed for the initial channalization of fretted channels on Mars [e.g., *Milton*, 1973; *Carr*, 2001]. If the sapping interpretation is correct, this suggests that SO_2 became liquid at a depth of 1 km or less when these canyons formed (perhaps continuing to the present). However, liquid SO_2 is modeled to usually occur at depths far below 4 km [*Leone and Wilson*, 1999], so liquid SO_2 at depths $\leq 1 \text{ km}$ may not be common. If sapping occurs,

it must rely on locally high geothermal energy to mobilize the liquid SO_2 . As the Tvashtar region currently is undergoing widespread volcanic activity, such geothermal energy is probably available. New high-resolution images of these canyons are planned for the I31 encounter (August 2001) to get a closer look at the morphology and to search for evidence of changes in the canyon walls.

3.4. Plastic Deformation

One of the possible emplacement mechanisms for the low-relief lobes extending from alcoves along type A slopes is solid-state flow. This could involve plastic deformation of material with interstitial volatiles (e.g., SO_2), somewhat analogous to glacial flow of water ice or ice-cored rock glaciers on Earth. Like liquid SO_2 sapping, this mechanism also would need a local concentration of geothermal energy to soften the SO_2 ice. Plastic deformation and “glacial” creep of interstitial water ice has been proposed for the formation of fretted terrain on Mars [e.g., *Sharp*, 1973; *Squyres*, 1978; *Lucchitta*, 1984; *Carr*, 1995]. It is claimed that in the Martian case plastic deformation of warm water ice would not necessarily cut channels or obviously streamline obstacles, and that ice might simply flow outward onto plains. Analogous processes on Io involving a different volatile would leave few lasting traces at the resolutions of the Galileo

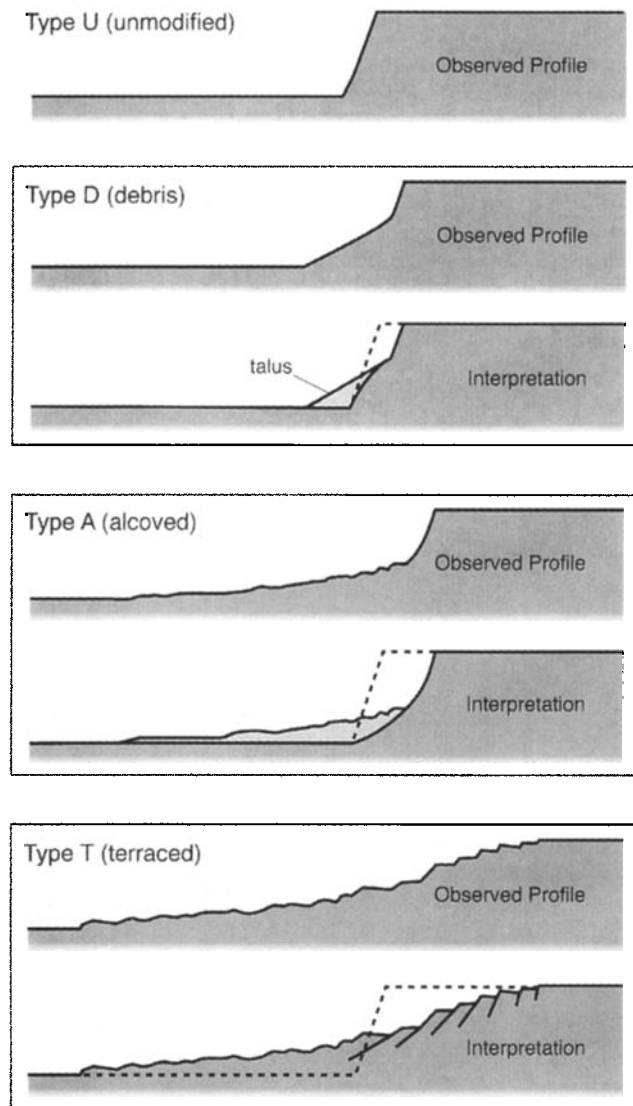


Figure 17. Stylized profiles of different slope types discussed in the text along with interpretive restorations of their evolution.

Tvashtar and Zal Montes observations, except flow lobes where movement was not topographically restricted. Similar morphologic arguments have been made for the hypothesis that some Martian terrains, such as the fretted terrain and large lobate aprons are substantially the result of warm deforming ice [e.g., *Squyres*, 1978; *Carr*, 1995]. An analogous process might be occurring on Io, but with a different “ice” volatile, that of SO_2 .

Could solid SO_2 flow downslope, or simply outward under its own weight, if sufficiently warmed from below? Although experimental stress-strain data for solid SO_2 is unknown to us, results from recent solid CO_2 deformation experiments imply that SO_2 may behave plastically at temperatures approaching its melting point (198 K). Figure 18 is a plot from *Durham et al.* [1999] showing the flow of several ices, including their recent results for CO_2 . Both SO_2 and CO_2 exhibit van der Waals intermolecular bonding. However, the configuration of CO_2 molecules is linear, and that of SO_2 is not, and so SO_2 will be more polar than CO_2 . Thus SO_2 ice may exhibit flow

behavior at temperatures normalized by their melting temperatures intermediate between H_2O and CO_2 . In any case, H_2O is apparently the stiffest cosmically abundant ice [e.g., *Durham et al.*, 1999]; hence SO_2 ice will flow more readily than H_2O ice at a given fraction of its melting temperature. As warm H_2O ice flows readily over very geologically short timescales, it is reasonable to assume sufficiently warm SO_2 ice will also.

3.5. Sublimation Degradation

Sublimation degradation is the result of disaggregation of relief-forming materials through the loss of their cohesive but ultimately volatile, rock-forming matrix or cement [*Moore et al.*, 1996]. Sublimation degradation has been proposed as an agent of kilometer-scale landform modification on Io [*Moore et al.*, 1996] and other Galilean satellites [*Moore et al.*, 1999; *Chuang and Greeley*, 2000]. Sublimation processes relevant to (noncometary) bodies containing volatiles in their surface layers have been modeled by a number of researchers [*Lebofsky*, 1975; *Purves and Pilcher*, 1980; *Squyres*, 1979; *Spencer* 1987; *Colwell et al.*, 1990; *Moore et al.*, 1996, 1999].

Moore et al. [1996], in their pre-Galileo study, proposed that in the case of Io’s polar regions (the area of highest-resolution coverage by the Voyager missions) only H_2S , sublimating from slopes that face the Sun and have thin lags, is volatile enough to cause the observed erosion. They concluded that SO_2 is not a viable candidate as an agent of erosion for high-latitude landforms. Models used by *Moore et al.* [1996], however, did indicate that SO_2 might sublimate quickly enough under a very thin (<5 cm), very low albedo (<0.05) lag to modify equatorial landforms on scales that might be observed in high-resolution (of order of 10 m pixel⁻¹) Galileo images. *Moore et al.* [1996] predicted that H_2S surface ice would be unambiguously detected on Io, particularly at the poles. This prediction, however, has not been borne out.

It is worth noting that a number of observations are consistent with the occasional presence of volcanically-released H_2S

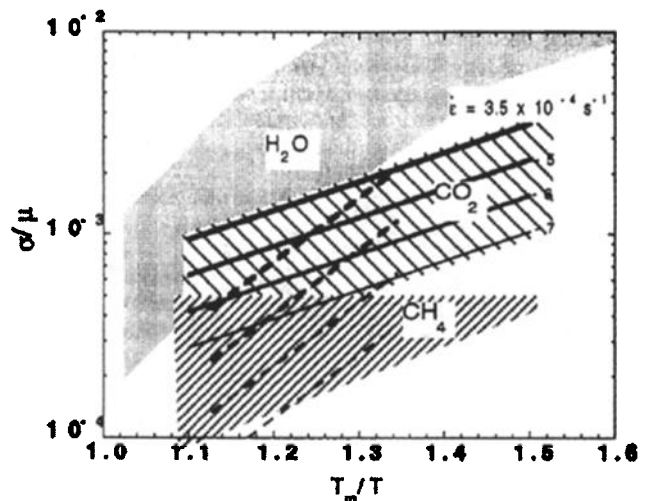


Figure 18. Plot from *Durham et al.* [1999] showing the flow of several ices. Stress is normalized by the shear modulus (μ) and the temperature is normalized by the melting temperature (T_m). SO_2 ice flow may fall between that of H_2O and CO_2 . See discussion in text.

but not stable H₂S frost deposits. *Nash and Howell* [1989] presented spectroscopic evidence for the transient occurrence of condensed H₂S on Io, but microwave observations failed to detect atmospheric H₂S, suggesting abundances below 10⁻¹⁰ bar [*Lellouch et al.*, 1990]. Observations by the Space Telescope Imaging Spectrograph (STIS) revealed enhanced H I Lyman- α emission near Io's poles, perhaps due to logenic hydrogen [*Roessler et al.*, 1999], but detailed analysis of the data has shown that it is reflected solar radiation attenuated by an SO₂ atmosphere concentrated near the equator [*Feldman et al.*, 2000]. *Russell and Kivelson* [this issue] present evidence for the temporally variable presence of H₂S⁺ in Io's exosphere. However, all these H₂S sightings give very little support for substantial H₂S deposits in the near surface.

As was noted in section 2.5 the amphitheatres among the ridges seen on Ot Mons (Figure 13) are apparently being enlarged by some erosion process, in which case the dark material seen on their floors may be erosional detritus. The appearance of amphitheater walls is consistent with sublimation-degradation [*Moore et al.*, 1996, 1999], as are the putatively identified differentially eroded layers seen at high resolution along the SE edge of the Isum plateau (Figure 15). As these features do not appear to be presently associated with local, very low albedo material, the role of SO₂ sublimation in their erosion is probably small.

3.6. Disaggregation From Chemical Decomposition

An erosional process that so far has had little discussion in Io studies is disaggregation from thermally induced chemical decomposition. *Hapke* [1989] and *Hapke and Graham* [1989] discussed S₂O and polysulfur oxide (PSO) and their potential contribution to spectra of Io surface materials. In the course of explaining why they thought S₂O and PSO might be present on Io's surface, they reviewed the temperature-dependent behavior of these materials. *Hapke* [1989] stated that S₂O and PSO could be formed when SO₂ gas is exposed to a dissociative environment such as the high temperatures associated with hot erupting magma. Recent observations [*McEwen et al.*, 1998] of very hot magmas on Io imply that the conditions for S₂O and PSO formation and deposition exist and may be common. *Hapke* [1989] notes that S₂O is stable if the temperature is less than about 115 K. As the temperature rises above this value, solid SO₂ does not sublime directly but instead disproportionates into S₂O and PSO. *Hapke* [1989] goes on to note that the transition from S₂O to PSO does not occur at a fixed temperature but over a range from ~115 to ~170 K. *Hapke and Graham* [1989] report that PSO can form on surfaces with temperatures as high as 300 K, and it can exist in a metastable state even at this temperature for months. *Hapke* [1989] comments that as the temperature rises from 115 K, PSO repolymerizes continuously into chains of increased S:O ratio, with attendant production of copious quantities of SO₂ and a considerable decrease in volume. Thus as PSO warms it disaggregates.

Hapke [1989] estimates that globally as much as 50 $\mu\text{m yr}^{-1}$ of S₂O from volcanoes may be deposited on Io, which would result in a layer 5 cm thick in 10³ years. Much thicker deposits might be expected in the vicinity of a long-erupting volcano. The S₂O/PSO deposits would probably be interlayered with dust-sized sulfur and silicate particles. S₂O/PSO-rich deposits could be susceptible to decomposition over a wide range of temperatures both due to solar insolation and geothermal heating. The rates of this decomposition would allow

the emplacement and subsequent decomposition of S₂O/PSO-rich layers on timescales compatible with the age of Io's surface and at a size scale that would be within the resolution of Galileo images.

Disaggregation from thermally induced chemical decomposition of solid S₂O/PSO should degrade landforms in a manner that resembles erosion from sublimation. If the disaggregation-causing heat is primarily solar, typical landforms that might be produced are rimless, irregularly shaped pits, unevenly retreating scarps [e.g., *Moore et al.*, 1996, 1999] and surfaces reminiscent of glacial ablation surfaces such as fields of cones or mounds [e.g., *Malin and Zimbelman*, 1986]. Geothermally induced S₂O/PSO disaggregation might also form pits, voids, and other collapse features. The erosional enlarged amphitheatres of the Ot Mons ridge crests (Figure 11) and the putatively identified differentially eroded layering and other surface textures seen in the along the SE edge of the Isum plateau (Figures 15 and 16) are good candidates for erosional expressions that are consistent with, though not proof of, S₂O/PSO disaggregation. The S₂O/PSO disaggregation hypothesis, however, is an intriguing explanation for erosional morphologies on Io, which could be attributable to sublimation but are not so ascribed due to the absence of a suitable volatile.

3.7. Implications for Volatile Abundances in Io's Upper Crust

Both the eroded layered terrain and the long-lived Prometheus-type plumes indicate that the upper crust of Io is rich in volatiles. *Hapke* [1989] proposed a model in which surface of Io is dominantly basaltic with only thin (~1 μm) coatings of PSO, S₂O, and SO₂, but *McEwen and Lunine* [1990] protested that such a model could not account for the volcanic activity and that volatiles must be much more abundant in Io's upper crust. This view is strengthened by evidence that Prometheus-type plumes are produced by interactions between silicate lava and near-surface SO₂ or sulfur in the surrounding plains extending hundreds of kilometers from the primary vents [*McEwen et al.*, 1998; *Kieffer et al.*, 2000; *Milazzo et al.*, this issue]. The eroded layered terrain imaged by Voyager in Io's south polar region also suggests a volatile-rich composition because the plateau materials appear to be completely removed in some manner [*Schaber*, 1982]. The high-resolution Galileo images support this impression, as discussed above. Both the Galileo and Voyager observations suggest more voluminous removal of plateau materials at high latitudes, but the low Sun images near the equator are very limited in coverage. We should expect greater volatiles at high latitudes where the surface is cooler, and this view is supported by mapping of forward scattering surface units interpreted as fresh SO₂ frost [*Geissler et al.*, this issue]. The Prometheus-type plumes have an equatorial concentration, but this is probably controlled by the lava eruption styles [*McEwen et al.*, 2000]. However, note that there are many long-lived eruptions that do not produce plumes, so presumably the upper crust has been depleted of volatiles in these regions. In summary, the evidence suggests that Io's upper crust is rich in volatiles, at least in places, at all latitudes.

4. Conclusions

1. We recognize four major slope types observed on a number of intermediate resolution (~250 m pixel⁻¹) images

and several additional textures on very high resolution (~10 m pixel⁻¹) images. Slopes and scarps on Io often show evidence of erosion, seen in the simplest form as alcove-carving slumps and slides at all scales. Many steep slopes on Io probably degrade through dry mass-wasting processes such as block release and brittle slope failure.

2. Sputtering probably plays no role in the erosion of Io's surface at the scale seen even in the highest-resolution images.

3. A sapping mechanism involving liquid SO₂, proposed by McCauley *et al.* [1979] to explain the irregular erosional scarps and bright deposits in layered terrains imaged by Voyager 1, may have formed the rectangular pattern of alcove-rimmed troughs in the Tvashtar plateau (classified as a manifestation of type A slopes in this paper), which resemble fretted plateau erosion on Mars. If the sapping explanation is correct, this suggests that SO₂ became liquid at a depth of 1 km or less when these canyons formed (perhaps continuing to the present). If sapping is, in fact, taking place, it must rely on locally high geothermal energy to mobilize the liquid SO₂.

4. Fretted erosion along portions of the Tvashtar plateau could also reflect plastic deformation and glacial flow of interstitial volatiles (e.g., SO₂) that exploit and enlarge structural patterns of weakness (e.g. joints and fractures), causing disaggregation and further back wasting into the plateau. This mechanism also relies on locally high geothermal energy to mobilize the volatile. Alcoves with lobes emerging from them seen elsewhere on the satellite may have formed in a similar manner.

5. The appearance of some slopes and near-slope surface textures seen in very high resolution images is consistent with erosional styles that could be attributed to sublimation-degradation. However, it is difficult to identify a suitable volatile (e.g., H₂S) that can sublimate fast enough to alter Io's youthful surface.

6. Disaggregation from chemical decomposition of solid S₂O and other polysulfur oxides may conceivably operate on Io. This mechanism could degrade landforms in a manner that resembles degradation from sublimation and at a rate comparable to that of resurfacing.

Acknowledgements. This investigation was funded by NASA's Galileo Project. We are grateful for the comments of an anonymous reviewer. Thanks goes to Pam Engebretson for her help with figure preparation.

References

- Bakker, J.P., and J.W.N. Le Heux, A remarkable new geomorphological law, *Proc. K. Ned. Akade. Wet., Ser. B Phys. Sci.*, 55, 399-410, 554-571, 1952.
- Carr, M.H., The Martian drainage system and the origin of networks and fretted channels, *J. Geophys. Res.*, 100, 7479-7507, 1995.
- Carr, M.H., Mars Global Surveyor observations of Martian fretted terrain, *J. Geophys. Res.*, in press, 2001.
- Chuang, F.C., and R. Greeley, Large mass movements on Callisto, *J. Geophys. Res.*, 105, 20,227-20,244, 2000.
- Coates, D.R., Landslide perspectives, *Rev. Eng. Geol.*, 3, 3-28, 1977.
- Colwell, J.E., B.M. Jakosky, B.J. Sandor, and S.A. Stern, Evolution of topography on comets. II. Icy craters and trenches, *Icarus*, 85, 205-215, 1990.
- Durham, W.B., S.H. Kirby, and L.A. Stern, Steady-state flow of solid CO₂: Preliminary results, *Geophys. Res. Lett.*, 26, 3493-3496, 1999.
- Feldman, P.D., D.F. Strobel, H.W. Moos, K.D. Retherford, B.C. Wolven, M.A. McGrath, F.L. Roesler, R.C. Woodward, R.J. Oliv-

- ersen, and G.E. Ballester, Lyman- α imaging of the SO₂ distribution on Io, *Geophys. Res. Lett.*, 27, 1787-1790, 2000.
- Geissler, P., A. McEwen, C. Phillips, D. Simonelli, R. Lopes-Gautier, and S. Doute, Galileo imaging of SO₂ frosts on Io, *J. Geophys. Res.*, this issue
- Hapke, B., The surface of Io: A new model, *Icarus*, 79, 56-74, 1989.
- Hapke, B., and F. Graham, Spectral properties of condensed phases of disulfur monoxide, polysulfur oxide, and irradiated sulfur, *Icarus*, 79, 47-55, 1989.
- Johnson, R.E., *Energetic Charged-Particle Interactions with Atmospheres and Surfaces*, *Phys. Chem. Space*, vol. 19, 232 pp., Springer-Verlag, New York, 1990.
- Johnson, T.V., and L.A. Soderblom, Volcanic eruptions on Io: Implications for surface evolution and mass loss, in *Satellites of Jupiter*, edited by D. Morrison, pp. 634-646, Univ. of Ariz. Press, Tucson, 1982.
- Johnson, T.V., D.L. Matson, D.L. Blaney, G.J. Veeder, and A. Davies, Stealth plumes on Io, *Geophys. Res. Lett.*, 22, 3293-3296, 1995.
- Kieffer, S.W., R. Lopes-Gautier, A. McEwen, W. Smythe, L. Keszthelyi, and R. Carlson, Prometheus: Io's wandering plume, *Science*, 288, 1204-1208, 2000.
- Klaassen, K.P., et al., Calibration and performance of the Galileo Solid-State Imaging system in Jupiter orbit, *Opt. Eng.*, 38, 1178-1199, 1999.
- Lebofsky, L.A., Stability of frosts in the solar system, *Icarus*, 25, 205-217, 1975.
- Lellouch, E., M. Belton, I. de Pater, S. Gulkis, and T. Encrenaz, Io's atmosphere from microwave detection of SO₂, *Nature*, 346, 639-641, 1990.
- Leone, G., and L. Wilson, The geothermal gradient of Io, *Lunar Planet. Sci. [CD-ROM]*, XXX, Abstract 1358, 1999.
- Lucchitta, B.K., Ice and debris in the fretted terrain, Mars, *Proc. Lunar Planet. Sci. Conf. 14th*, Part 2, *J. Geophys. Res.*, 89, suppl., B409-B418, 1984.
- Malin, M.C., Mass movements on Venus: Preliminary results from Magellan cycle 1 observations, *J. Geophys. Res.*, 97, 16,337-16,352, 1992.
- Malin, M.C., and D. Dzurisin, Landform degradation on Mercury, the Moon, and Mars: Evidence from crater depth/diameter relationships, *J. Geophys. Res.*, 82, 376-388, 1977.
- Malin, M.C., and J.R. Zimbelman, Surface morphology of cometary nuclei, *Lunar Planet. Sci.*, XVII, 512-513, 1986.
- McCauley, J.F., B.A. Smith, and L.A. Soderblom, Erosional scarps on Io, *Nature*, 280, 736-738, 1979.
- McEwen, A.S., and J.I. Lunine, Comment on "The surface of Io: A new model" by Bruce Hapke, *Icarus*, 84, 268-274, 1990.
- McEwen, A.S., et al., High-temperature silicate volcanism on Jupiter's moon Io, *Science*, 281, 87-90, 1998.
- McEwen, A.S., et al., Galileo at Io. Results from high-resolution imaging, *Science*, 288, 1193-1198, 2000.
- Milazzo, M.P., L.P. Keszthelyi, and A.S. McEwen, Observations and initial modeling of lava-SO₂ interactions at Prometheus, Io, *J. Geophys. Res.*, this issue.
- Milton, D.J., Water and processes of degradation in the Martian landscape, *J. Geophys. Res.*, 78, 4037-4047, 1973.
- Moore, J.M., M.T. Mellon, and A.P. Zent, Mass wasting and ground collapse in terrains of volatile-rich deposits as a solar system-wide geological process: The pre-Galileo view, *Icarus*, 122, 63-78, 1996.
- Moore, J.M., et al., Mass movement and landform degradation on the icy Galilean satellites: Results from the Galileo nominal mission, *Icarus*, 140, 294-312, 1999.
- Nash D.B., and R.R. Howell, Hydrogen sulfide on Io: Evidence from telescopic and laboratory infrared spectra, *Science* 244, 454-457, 1989.
- Pappalardo, R. T., and R. Greeley, A review of the origins of sub-parallel ridges and troughs: Generalized morphological predictions from terrestrial models, *J. Geophys. Res.*, 100, 18,985-19,007, 1995.
- Purves, N.G., and C.B. Pilcher, Thermal migration of water on the Galilean satellites, *Icarus*, 43, 51-55, 1980.
- Radebaugh, J., L.P. Keszthelyi, A. S. McEwen, E.P. Turtle, W.L. Jaeger, M. Milazzo, and the Galileo SSI Team, Paterae on Io: A new type of volcanic caldera?, *J. Geophys. Res.*, this issue.
- Roessler, F.L., H.W. Moos, R.J. Oliverson, R.C. Woodward Jr., K.D. Retherford, F. Scherb, M.A. McGrath, W.H. Smyth, P.D. Feld-

- man, and D.F. Strobel, Far-ultraviolet imaging spectroscopy of Io's atmosphere with HST/STIS, *Science* 283, 353-357, 1999
- Russell, C.T., and M.G. Kivelson, Evidence for sulfur dioxide, sulfur monoxide, and hydrogen sulfide in the Io exosphere, *J. Geophys. Res.*, this issue.
- Schaber, G.G., The geology of Io, in *Satellites of Jupiter*, edited by D. Morrison, pp. 556-597, Univ. of Ariz. Press, Tucson, 1982.
- Schenk, P.M., and M.H. Bulmer, Origin of mountains on Io by thrust faulting and large-scale mass movements, *Science*, 279, 1514-1517, 1998.
- Selby, M. J., *Hillslope Materials and Processes*, 2nd ed., pp. 365-369, Oxford Univ. Press, New York, 1993.
- Sharp, R.P., Mars: Fretted and chaotic terrains, *J. Geophys. Res.*, 78, 4073-4083, 1973.
- Sharpe, C.F.S., *Landslides and Related Phenomena*, 137 pp., Cooper Square, New York, 1939.
- Spencer, J.R., Thermal segregation of water ice on the Galilean satellites, *Icarus*, 69, 297-313, 1987.
- Squyres, S.W., Martian fretted terrain: Flow of erosional debris, *Icarus*, 34, 600-613, 1978.
- Squyres, S.W., The evolution of dust deposits in the Martian north polar region, *Icarus*, 40, 244-261, 1979.
- Turtle, E. P., et al., Mountains on Io: High-resolution Galileo observations, initial interpretations, and formation models, *J. Geophys. Res.*, this issue.
- Varnes, D.J., Landslide types and processes, in *Landslides and Engineering Practice*, edited by E.B. Eckel, pp. 20-47, Nat. Acad. of Sci., Nat. Res. Counc. Highway Res. Board, Washington, D. C., 1958.
- Varnes, D.J., Slope movement types and processes, in *Landslide, Analysis, and Control*, edited by R.L. Shuster and R.J. Kriszek, pp. 11-33, Nat. Acad. of Sci., Nat. Res. Counc. Transp. Res. Board, Washington, D. C., 1978.
- F.C. Chuang, Department of Geological Sciences, Arizona State University, Tempe, AZ 85287.
- J.W. Head III and B.E. Nixon, Department of Geological Sciences, Brown University, Box 1846, Providence, RI 02912. (james.head.III@brown.edu)
- A.S. McEwen, M. Milazzo, and E.P. Turtle, Lunar and Planetary Laboratory, University of Arizona, 1629 East University Blvd., Tucson, AZ 85721. (mcewen@pirl.lpl.arizona.edu; mmilazzo@pirlmail.lpl.arizona.edu; turtle@pirlmail.lpl.arizona.edu)
- J.M. Moore, Space Sciences Division, NASA Ames Research Center, MS 245-3, Moffett Field, CA 94035-1000. (jmoore@mail.arc.nasa.gov)
- R.T. Pappalardo, Astrophysical and Planetary Sciences Department, Campus Box 392, University of Colorado, Boulder, CO 80309-0392. (pappalardo@lasp.colorado.edu)
- P.M. Schenk, Lunar and Planetary Institute, 3600 Bay Area Boulevard, Houston, TX 77058. (schenk@lpi.usra.edu)
- R.J. Sullivan, Center for Radiophysics and Space Research, Cornell University, 308 Space Sciences Building, Ithaca, NY 14853-6801. (sullivan@cuspi.f.tn.cornell.edu)

(Received September 5, 2000; revised February 15, 2001; accepted March 12, 2001.)